

Proceedings of the Korean Nuclear Society Spring Meeting
Cheju, Korea, May 2001

Numerical Stability Analysis and Evaluation of Stability Enhancing Interfacial Pressure Force Model

Ho Gon Lim, Kyung Doo Kim, Won Jae Lee

Korea Atomic Energy Research Institute
P. O. Box 105, Yusung, 305-606
Taejeon, Korea

Un Chul Lee

Seoul National University
San56-1 shilnlm, Kwanak, Seoul, Korea

Abstract

In order to overcome the ill-posedness of a typical two-fluid model, a hyperbolic equation system has been developed by introducing an interfacial pressure force in phasic momentum equations. The interfacial pressure force for the present model is derived by characteristic analysis under the assumption of isentropic compressible flow condition. The potential impact of the present model on numerical stability has been examined by Von-Neumann stability analysis. The obvious improvement in numerical stability has been found when a semi-implicit time advancement scheme with implicit treatment of the interfacial pressure force term is used. Numerical experiments using the pilot code have also been shown that the propagation of void wave perturbation and the water faucet flow are well predicted without distortion.

1.Introduction

For thermal-hydraulic modeling of two-phase flow systems, six-equation models, which contain mass, energy and momentum conservation equations for each phase, are commonly used in codes for nuclear reactor safety analyses. Typical six-equation models assume that the pressures of liquid, vapor and interface are identical, a so-called single-pressure model, to eliminate the requirement of an additional closure equation. Unfortunately, typical two-phase flow models with a single pressure assumption possess complex characteristics that result in the equation system being ill-posed [1]. As a result, typical six-equation models may cause

the unbounded growth of instabilities. With the aid of lower order frictional term such as interfacial drag, this system can describe the two-phase flow behavior in coarse mesh by which short wavelength solution component are not represented. However, as the mesh size is refined, this system has short wavelength instability due to its non-hyperbolic characteristic.

Trapp has mentioned in his paper that the reasons are mainly considered due to the assumption of equal pressures between phases and the failure to model the correlations of the velocity fluctuations in momentum equations. The interfacial momentum transfer terms such as surface tension, tangential phasic velocity differences, etc. are disappeared in the momentum equations by this assumption. Many authors have shown that two-fluid model can achieve hyperbolic system by including the effect of unequal pressure between phases [1977, Stuhmiller, 1978, Ramshaw, 1985, Ransom, 1986, Holm, 1998, Lee]. Ramshaw and Trapp proposed sigma equation system by introducing surface tension in the stratified flow at the slab geometry as phasic pressures constraint. They showed that their equations have real eigenvalues and therefore, are hyperbolic. Also, They illustrated that their system is stable at the range of short wavelength by linear stability analysis. Since pressure constraints in general flow structures are so complicated that this model cannot be applied other geometries except stratified flow in slab geometry. Stuhmiller introduced the interfacial pressure force. He studied interfacial pressure force for bubbly flow under incompressible flow condition. By characteristic analysis, he has found the minimum value of interfacial pressure force, which makes the system hyperbolic. CATHARE [8] employed this model as its field equations. However, the assumption used is not applicable for a general two-phase flow condition. Noticeable model was proposed by Ransom, et al. They noticed that transverse conservation relation must be included to model separated flow condition. For separated flow, they introduced the transverse void transport and momentum transport equations and showed that their system has a suitable eigenvalues set. Their system was also shown to be stable by dispersion analysis and numerical comparison with single pressure model. It is thought that this approach is desirable for realistic two-phase flow calculation. However, conservation relations of transverse direction for all flow regimes must be established to implement into codes. Recently, Lee proposed the pressure jump model to account for the pressure difference between phases based on the notion of surface tension. By characteristic analysis, he showed that his model has real characteristics. However, this model needs an additional closure relation for interfacial area intensity, which has not been established yet.

Several authors thought that ill-posedness of a basic two-fluid model are due to lack of appropriate terms which must be included to describe real physical phenomena in two-phase flow [1979, Drew, 1980, Arai, 1985, No]. Drew, et al. have searched the proper form of virtual mass force on the basis of objectivity of interfacial momentum transfer. And No and Kazimi studied an effect of virtual mass force under incompressible conditions. They showed that the system of equations has two real eigenvalues by inclusion of virtual mass force with proper coefficient. Numerical stability is also illustrated by linearized Von-Neumann stability analysis under the incompressible condition. However, it is not certain that hyperbolic system is maintained for general situations such as compressible flow condition. Arai studied the viscous force effect on two-fluid model. By Characteristic analysis, he showed that his system is hyperbolic. In a strict definition of hyperbolic system, his model is not a hyperbolic one because characteristic polynomial has quadruple roots of zero. Also if the original model proposed in his model is used, increase of two additional equations that make his model first

order differential form will increase calculation time which is not desirable in fast running request of present system code.

A hyperbolic equations system was proposed by introducing a new interfacial pressure force model into the single-pressure two-fluid equations[17]. The proper value of interfacial pressure force was derived by characteristic analysis. Because an assumption for incompressible condition, which used in previous attempts, is not suitable for a real two-phase flow system, isentropic condition was assumed in this study. Numerical Stability analysis is performed for the semi-implicit differencing widely used in reactor safety analysis code in the sense of Von Neumann and also numerical experiment is carried out using pilot code which is developed using semi-implicit time differencing.

2. Interfacial Pressure Force

The two-phase flow equation system that involves the phasic interfacial pressure force terms is considered. For isentropic conditions, the expanded mass and momentum equations can be written as:

$$r_g \frac{\partial a_g}{\partial t} + \frac{a_g}{c_g^2} \frac{\partial p}{\partial t} + r_g v_g \frac{\partial a_g}{\partial x} + \frac{a_g v_g}{c_g^2} \frac{\partial p}{\partial x} + r_g a_g \frac{\partial v_g}{\partial x} = 0 \quad (1)$$

$$-r_f \frac{\partial a_f}{\partial t} + \frac{a_f}{c_f^2} \frac{\partial p}{\partial t} - r_f v_f \frac{\partial a_f}{\partial x} + \frac{a_f v_f}{c_f^2} \frac{\partial p}{\partial x} + r_f a_f \frac{\partial v_f}{\partial x} = 0 \quad (2)$$

$$a_g r_g \frac{\partial v_g}{\partial t} + a_g r_g v_g \frac{\partial v_g}{\partial x} + a_g \frac{\partial p}{\partial x} + Dp_g \frac{\partial a_g}{\partial x} = 0 \quad (3)$$

$$a_f r_f \frac{\partial v_f}{\partial t} + a_f r_f v_f \frac{\partial v_f}{\partial x} + a_f \frac{\partial p}{\partial x} - Dp_f \frac{\partial a_f}{\partial x} = 0 \quad (4)$$

where subscripts 'g' and 'f' represent the gas and liquid phase, respectively, and Δp_g and Δp_f represent the interfacial pressure forces. To find out the appropriate value for Δp , which can make the equation system hyperbolic, the characteristic analysis is performed. Equations (1) through (4) can be written in a matrix form as

$$A \frac{\partial v}{\partial t} + B \frac{\partial v}{\partial x} = 0 \quad (5)$$

$$\text{Where } A = \begin{pmatrix} \mathbf{r}_g & \frac{\mathbf{a}_g}{c_g^2} & 0 & 0 \\ -\mathbf{r}_f & \frac{\mathbf{a}_f}{c_f^2} & 0 & 0 \\ 0 & 0 & \mathbf{a}_g \mathbf{r}_g & 0 \\ 0 & 0 & 0 & \mathbf{a}_f \mathbf{r}_f \end{pmatrix}$$

$$B = \begin{pmatrix} \mathbf{r}_g v_g & \frac{\mathbf{a}_g v_g}{c_g^2} & \mathbf{r}_g \mathbf{a}_g & 0 \\ -\mathbf{r}_f v_f & \frac{\mathbf{a}_f v_f}{c_f^2} & 0 & \mathbf{r}_f \mathbf{a}_f \\ \mathbf{D}p_g & \mathbf{a}_g & \mathbf{a}_g \mathbf{r}_g v_g & 0 \\ -\mathbf{D}p_f & \mathbf{a}_f & 0 & \mathbf{a}_f \mathbf{r}_f v_f \end{pmatrix}, \text{ and } v = (\mathbf{a}_g \quad p \quad v_g \quad v_f)^T$$

For equation (5) to be hyperbolic, the characteristic equation must have four distinct real roots. The characteristic equation can be reduced to the following form:

$$\mathbf{a}_f c_g^2 [\mathbf{D}p_g - \mathbf{r}_g (1 - v_g)^2] [c_f^2 - (1 - v_f)^2] + \mathbf{a}_g c_f^2 [\mathbf{D}p_f - \mathbf{r}_f (1 - v_f)^2] [c_g^2 - (1 - v_g)^2] = 0 \quad (6)$$

Equation (6) is a fourth order polynomial and since it is not easy to directly solve the characteristics, equation (6) is transformed to a parametric form by assuming the same interfacial pressure difference, i.e., $\Delta p_g = \Delta p_f$

$$X = (1 - v_g)^2, Y = (1 - v_f)^2 \quad (7)$$

$$(X - \mathbf{x}_1)(Y - \mathbf{x}_2) = \mathfrak{R} \quad (8)$$

where

$$\mathbf{x}_1 = \frac{\mathbf{a}_f c_g^2 c_f^2 \mathbf{r}_g + \mathbf{a}_g c_f^2 \mathbf{D}p_f}{\mathbf{a}_f c_g^2 \mathbf{r}_g + \mathbf{a}_g c_f^2 \mathbf{r}_f}, \mathbf{x}_2 = \frac{\mathbf{a}_g c_f^2 c_g^2 \mathbf{r}_f + \mathbf{a}_f c_g^2 \mathbf{D}p_g}{\mathbf{a}_f c_g^2 \mathbf{r}_g + \mathbf{a}_g c_f^2 \mathbf{r}_f}, \mathfrak{R} = \frac{\mathbf{a}_g \mathbf{a}_f c_f^2 c_g^2 (\mathbf{D}p_g - \mathbf{r}_g c_g^2)(\mathbf{D}p_f - \mathbf{r}_f c_f^2)}{(\mathbf{a}_f c_g^2 \mathbf{r}_g + \mathbf{a}_g c_f^2 \mathbf{r}_f)^2}$$

Equations (8) and (9) represent parabola inclined by 45 degrees and hyperbola, respectively. These two curves must have four intersections in the region of positive X and Y in order to have four real distinct roots. Figure 1 shows the graphical representation of these curves. Since we are looking for a small interfacial pressure force which does not distort the solution of typical two-phase flow equations and enhances the stability, we put an assumption such that lower portion of hyperbola must intersect with parabola in the region of $X \in [0, (v_g - v_f)^2]$.

For simplicity, we have examined the magnitude of the interfacial pressure differences when

the intersections occur at $X=0$ and $(v_g - v_f)^2$. From the sensitivity study, it was found that most of minimum values occurred at the position of $X=(v_g - v_f)^2$ while a few can occurred $X=0$ for the small void fractions. Therefore, the magnitude of interfacial pressure force was determined to choose the small one between two values.

The interfacial pressure difference is conservatively determined by choosing the smaller one such as:

$$\Delta p = \text{Min} \left(\frac{\mathbf{a}_f \mathbf{r}_g c_g^2 (v_g - v_f)^2}{c_g^2 - \mathbf{a}_g (v_g - v_f)^2}, \frac{\mathbf{a}_g \mathbf{r}_f c_f^2 (v_g - v_f)^2}{c_f^2 - \mathbf{a}_f (v_g - v_f)^2} \right) \quad (9)$$

3.Numerical Stability Analysis

To investigate the numerical stability of the new model, a linearized Von-Neumann stability analysis was performed. The source terms including frictional drag are not considered to investigate the influence on stability of present model by excluding the influence by these terms. It can be shown that inclusion of the phasic energy equations requires the convective limits, often called Courant limits, for each phase satisfied. Thus, the phasic energy equations are neglected in this stability analysis under the condition that the convective limits are obeyed. The stability analysis has been carried out for the semi-implicit time difference on a staggered spatial mesh, because this difference scheme is widely used in major thermal-hydraulic codes and has advantages in computational efficiency. The interfacial pressure difference terms in discretized phasic momentum equations are treated implicitly to enhance the numerical stability. The resultant phasic mass and momentum equations can be written as:

vapor mass:

$$\begin{aligned} \mathbf{r}_g \left\{ \frac{\mathbf{a}_{g,j}^{i+Dt} - \mathbf{a}_{g,j}^i}{Dt} \right\} + \frac{\mathbf{a}_{g,j}^i}{c_g^2} \left\{ \frac{p_j^{i+Dt} - p_j^i}{Dt} \right\} + \mathbf{r}_g v_{g,j+1/2}^{i+Dt} \left\{ \frac{\mathbf{a}_{g,j}^i - \mathbf{a}_{g,j-1}^i}{Dx} \right\} \\ + \frac{\mathbf{a}_{g,j}^i v_{g,j+1/2}^{i+Dt}}{c_g^2} \left\{ \frac{p_j^i - p_{j-1}^i}{Dx} \right\} + \mathbf{r}_g \mathbf{a}_{g,j}^i \left\{ \frac{v_{g,j+1/2}^{i+Dt} - v_{g,j-1/2}^{i+Dt}}{Dx} \right\} = 0 \end{aligned} \quad (10)$$

liquid mass:

$$\begin{aligned} \mathbf{r}_f \left\{ \frac{\mathbf{a}_{f,j}^{i+Dt} - \mathbf{a}_{f,j}^i}{Dt} \right\} + \frac{\mathbf{a}_{f,j}^i}{c_g^2} \left\{ \frac{p_j^{i+Dt} - p_j^i}{Dt} \right\} + \mathbf{r}_f v_{f,j+1/2}^{i+Dt} \left\{ \frac{\mathbf{a}_{f,j}^i - \mathbf{a}_{f,j-1}^i}{Dx} \right\} \\ + \frac{\mathbf{a}_{f,j}^i v_{f,j+1/2}^{i+Dt}}{c_g^2} \left\{ \frac{p_j^i - p_{j-1}^i}{Dx} \right\} + \mathbf{r}_f \mathbf{a}_{f,j}^i \left\{ \frac{v_{f,j+1/2}^{i+Dt} - v_{f,j-1/2}^{i+Dt}}{Dx} \right\} = 0 \end{aligned} \quad (11)$$

vapor momentum:

$$\begin{aligned} \mathbf{r}_g \mathbf{a}_{g,j+1/2}^i \left\{ \frac{v_{g,j+1/2}^{i+Dt} - v_{g,j+1/2}^i}{Dt} \right\} + \mathbf{r}_g \mathbf{a}_{g,j+1/2}^i v_{g,j+1/2}^{i+Dt} \left\{ \frac{v_{g,j+1/2}^i - v_{g,j-1/2}^i}{Dx} \right\} \\ + \mathbf{a}_{g,j+1/2}^i \left\{ \frac{p_{j+1}^{i+Dt} - p_j^{i+Dt}}{Dx} \right\} + Dp \left\{ \frac{\mathbf{a}_{g,j+1}^{i+Dt} - \mathbf{a}_{g,j}^{i+Dt}}{Dx} \right\} = 0 \end{aligned} \quad (12)$$

liquid momentum:

$$\begin{aligned}
& \mathbf{r}_f \mathbf{a}'_{f,j+1/2} \left\{ \frac{v'_{f,j+1/2} - v'_{f,j+1/2}}{Dt} \right\} + \mathbf{r}_f \mathbf{a}'_{f,j+1/2} v'_{f,j+1/2} \left\{ \frac{v'_{f,j+1/2} - v'_{f,j-1/2}}{Dx} \right\} \\
& + \mathbf{a}'_{f,j+1/2} \left\{ \frac{p'_{j+1} - p'_{j+1}}{Dx} \right\} - Dp \left\{ \frac{a'_{g,j+1} - a'_{g,j}}{Dx} \right\} = 0
\end{aligned} \tag{13}$$

Perturbed linear system of equations is obtained by expressing each variable as a perturbation from a fixed reference state. Thus, any parameter Ψ_j^t is expressed as $\Psi_j^t = \Psi + \mathbf{d}\Psi_j^t$. Then, it is assumed that each perturbation can be expressed as a Fourier component of the form $\mathbf{dY}_j^t \approx \mathbf{dY}_j^t e^{ikx_j}$. Substituting these perturbation terms into perturbed linear system of equations yields the linear system represented by the amplitude of the perturbations. In case that \mathbf{U} is a vector containing four amplitudes of the perturbations, $\mathbf{d}\mathbf{a}_g$, $\mathbf{d}v_g$, $\mathbf{d}v_f$, and $\mathbf{d}p$, the this linear system can be written in the form of $\mathbf{A}\mathbf{U}^{t+Dt} = \mathbf{B}\mathbf{U}^t$. The condition for stability is that the eigenvalues of the amplification matrix $\mathbf{G} = \mathbf{A}^{-1}\mathbf{B}$ must be equal to or less than 1. The eigenvalues are the roots of the characteristic polynomial equation, $|\mathbf{A}\mathbf{I} - \mathbf{B}| = 0$, that is:

$$\left\{ \mathbf{L}_f^2 \mathbf{L}_g^2 + \bar{\mathcal{E}}^2 k'^2 \mathbf{I}^2 (\mathbf{L}_f^2 + \mathbf{e}^2 \mathbf{L}_g^2) \right\} + \mathbf{k}_p \bar{\mathcal{E}}^2 k'^2 \mathbf{I}^2 \left\{ \frac{\mathbf{a}_g}{\mathcal{E}_g^2} \mathbf{L}_g^2 + \frac{\mathbf{a}_f}{\mathcal{E}_f^2} \mathbf{L}_f^2 + k'^2 \mathbf{I}^2 \right\} = 0 \tag{14}$$

where $\mathbf{L}_k \equiv \mathbf{I} - \mathbf{l} + \tilde{v}_k$, $\mathbf{e}^2 \equiv \frac{\mathbf{a}_f \mathbf{r}_g}{\mathbf{a}_g \mathbf{r}_f}$, $\mathcal{E}_k \equiv c_k \frac{Dt}{Dx}$, $\mathbf{k}_p \equiv \frac{Dp}{\mathbf{a}_g \mathbf{r}_f} \frac{Dt^2}{Dx^2}$, $\bar{\mathcal{E}}^2 \equiv \frac{\mathcal{E}_g^2 \mathcal{E}_f^2}{\mathcal{E}_g^2 + \mathbf{e}^2 \mathcal{E}_f^2}$

$$\tilde{v}_k = v_k \frac{\Delta t}{\Delta x} (1 - e^{-ik\Delta x}), \quad k' = 2 \sin(kDx/2)$$

This fourth order characteristic polynomial is too complicated to determine the spectral radius analytically. To verify the effect of the present model, the spectral radius contour for the present model and virtual mass force model together with basic model are depicted in figures 1 and 2 for the representative conditions of compressibility and incompressibility, respectively. In the figures 1 and 2, for small and large phasic sonic speeds, which imply compressible and incompressible conditions, respectively, the spectral radius contours within the convective limit are shown for the present model. In both cases, the spectral radius of the new model is less than one. Whereas, the basic model shows only narrow stable region where the phasic velocity difference is small and in the case of the virtual mass model, the stable region is broadened compared to the basic model by the inclusion of virtual mass force. However, unstable regions still appear as the phasic velocity difference becomes larger. In general, stable region of virtual mass force are broadened with the increase of virtual mass coefficient from the sensitivity study while large value of this coefficient can distort the nature of two-fluid model. Consequently, the interfacial pressure force significantly enhances the numerical stability.

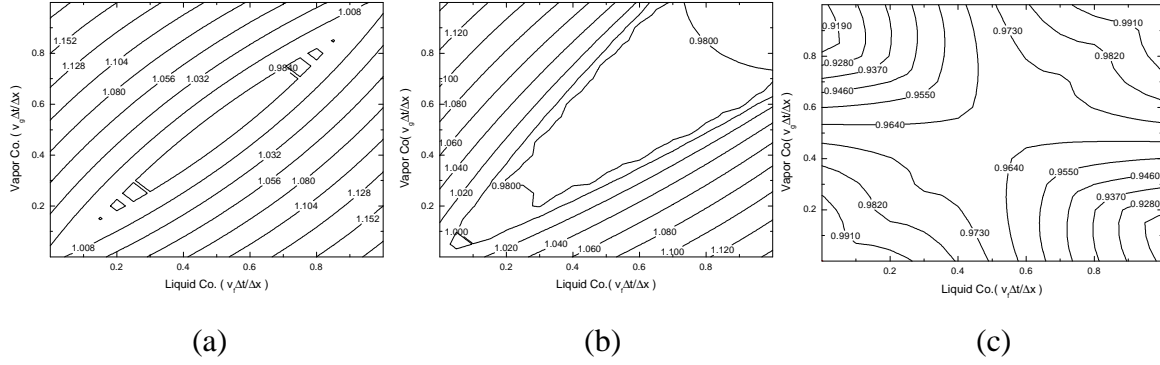


Figure 1 Amplification Matrix Spectral Radius Contour for the Compressible Flow Condition

$$\mathcal{G}_g = 1, \mathcal{G}_l = 5, kDx = p/6, e = 1, a_g = 0.5$$

(a) Basic model, (b) Virtual mass force model ($C_v = 1.0$), (c) New model

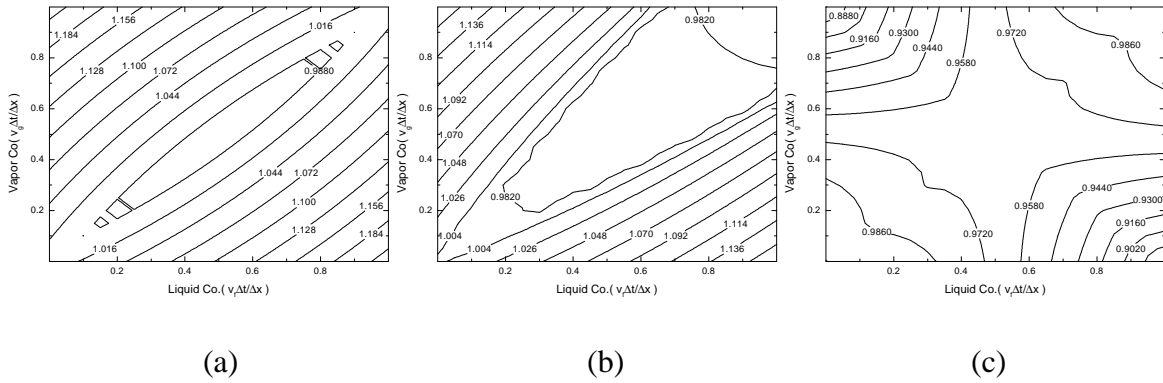


Figure 3 Amplification Matrix Spectral Radius Contour for the Incompressible Flow Condition

$$\mathcal{G}_g = 10^3, \mathcal{G}_l = 5 \times 10^3, kDx = p/6, e = 1, a_g = 0.5$$

(a) Basic model, (b) Virtual mass force model ($C_v = 1.0$), (c) New model

4. Numerical Experiments

The new hyperbolic model described here was implemented in a prototype code with the same numerical scheme used in the numerical stability analysis. After differencing for time and space, the new time values of the phasic velocities can be written as functions of the new time values of pressure and the void fraction. Substituting them into the mass and energy equations results in two equations involving the new time values of pressure and void fractions. For the flow system with N computational volumes, a $2N \times 2N$ system of linear equations can be obtained for the new time pressure and void fraction. A 2×2 block tridiagonal matrix solver (Anderson, 1984) is used for $(p_L^{n+1} - p_L^n)$ and $(a_{L,g}^{n+1} - a_{L,g}^n)$ for each volume. The new time values of pressures and void fractions are then substituted into the differenced momentum equations to solve for the new time phasic velocities. The new time

velocities are then used to obtain the new time vapor and liquid energy $u_{g,l}^{n+1}$, $u_{f,l}^{n+1}$.

To examine the stability and accuracy of present model, a wave perturbation and Faucet problems have been simulated and the results are compared with those for the basic two fluid model with virtual mass force in their momentum equations. As in the case of numerical stability analysis, frictional drag was not included. A horizontal pipe of 11m is selected as test geometry and discretized into 96 volumes. Since we are mainly concerned with the short wavelength instability that is critical problem for non-hyperbolic system, pipe was finely discretized to investigate this instability.

4.1 Wave Perturbation Problem

It is well known that if the system of equations is hyperbolic and a consistent numerical scheme is adapted, a perturbation must not be amplified or be damped along with its propagation. The simulations were carried out for two kinds of waves, having different wavelengths. Pipe is initially filled with saturated liquid and vapor with constant void fraction of 0.5. The initial liquid and vapor velocities are 1 m/s and 0.1m/s respectively. As shown in Figures 3 through 6, the perturbed void and pressure waves are damped properly in the present model as the wave propagates. On the contrary, the basic model shows unstable wave propagation. Especially for the void perturbation, the wave is amplified continuously and is not damped out. For the pressure wave perturbation, wave is propagated with the phasic sonic speed and is continuously damped for the present model. In the basic model, the pressure perturbation is damped as in the new model. However, for long wave perturbation, the pressure wave is not propagated well as in the present model. It is thought that these behaviors of the basic model are due to partially elliptic characteristic of this model. From these results, it is obvious that the new model with the interfacial pressure difference term is more stable.

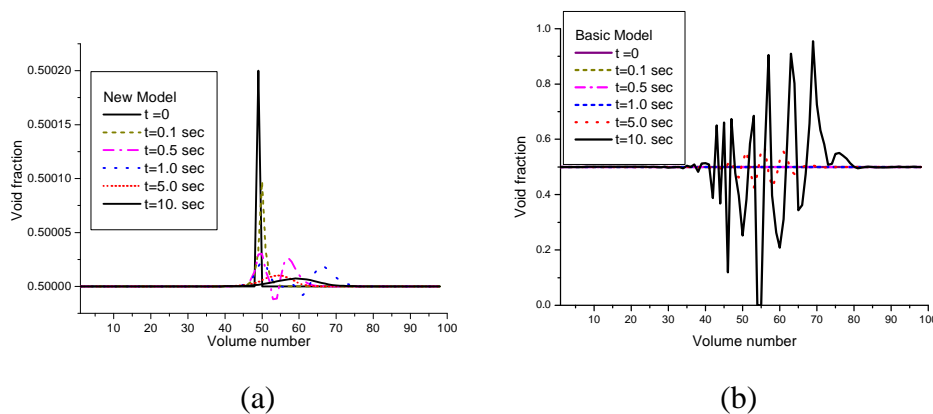
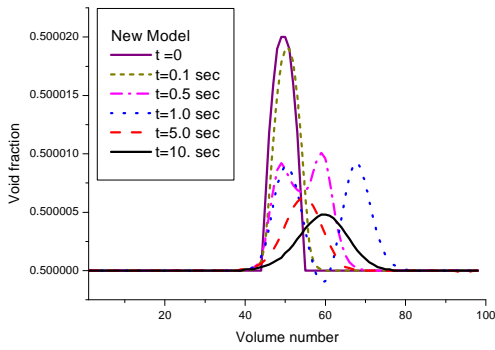
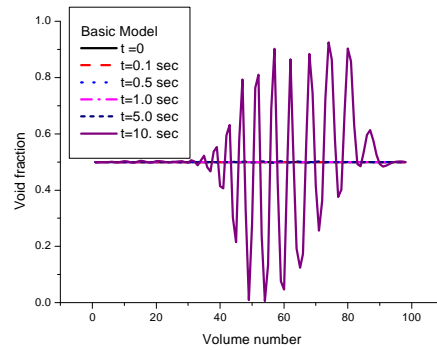


Figure 3 Short Wavelength Void Perturbation (perturbation wavelength: $l \times \Delta x$)
 $v_f = 1m / sec, v_g = 0.1m / sec$ (a) New Model (b) Basic Model

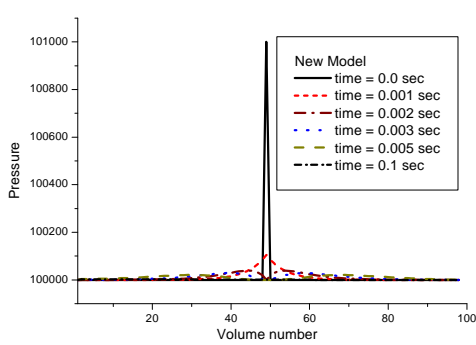


(a)

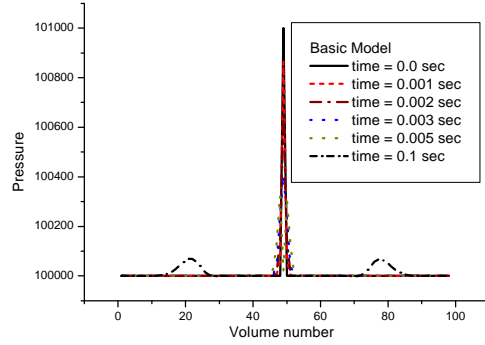


(b)

Figure 4 Long Wavelength Void Perturbation (perturbation wavelength: $11 \times D_x$)
 $v_f = 1m / sec, v_g = 0.1m / sec$ (a) New Model (b) Basic Model

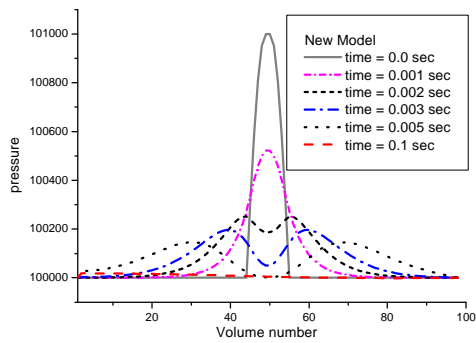


(a)

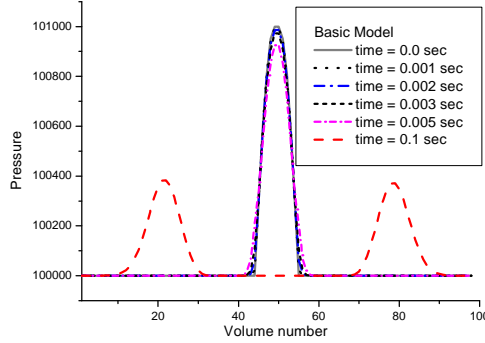


(b)

Figure 5 Short Wavelength Pressure Perturbation (perturbation wavelength: $1 \times D_x$)
 $v_f = 1m / sec, v_g = 0.1m / sec$ (a) New Model (b) Basic Model



(a)



(b)

Figure 6 Long Wavelength Pressure Perturbation (perturbation wavelength: $11 \times D_x$)
 $v_f = 1m / sec, v_g = 0.1m / sec$ (a) New Model (b) Basic Model

5.2 Water Faucet Problem

Since the present model was developed to enhance the stability of two-fluid model, the side effects that make the original features of two-fluid model distorted may occur. In this numerical experiment, the accuracy of the present model is tested. It is difficult to choose a benchmark problem since most two-phase flow problems do not have an analytic solution. Ransom has developed a two-phase benchmark problem, which has an analytic solution [12]. In his problem, the only driving force is gravity and frictional drags are ignored. The simulated pipe is a vertical channel with 96 volumes and is about 11m high. At the start of the simulation, water falls into the pipe with an initial velocity of 10m/s at the top of entrance. The water, then, is accelerated by gravity. As shown in figure 7, the result of the new model has good agreement with the exact solution. Broadening of the void fraction profile at the front is thought to be due to numerical diffusion. The result of virtual mass force model was distorted compared with exact solution. In this test, virtual mass force in basic model is used same as RELAP5/MOD3. In Benchmark test for RELAP5/MOD2[], they have eliminated virtual mass force terms which is not suitable for non-dispersed flow condition such as Faucet problem. Since the virtual mass force are mainly concerned with dispersed flow such as bubbly flow or droplet flow[], the results without virtual mass force are more reasonable.

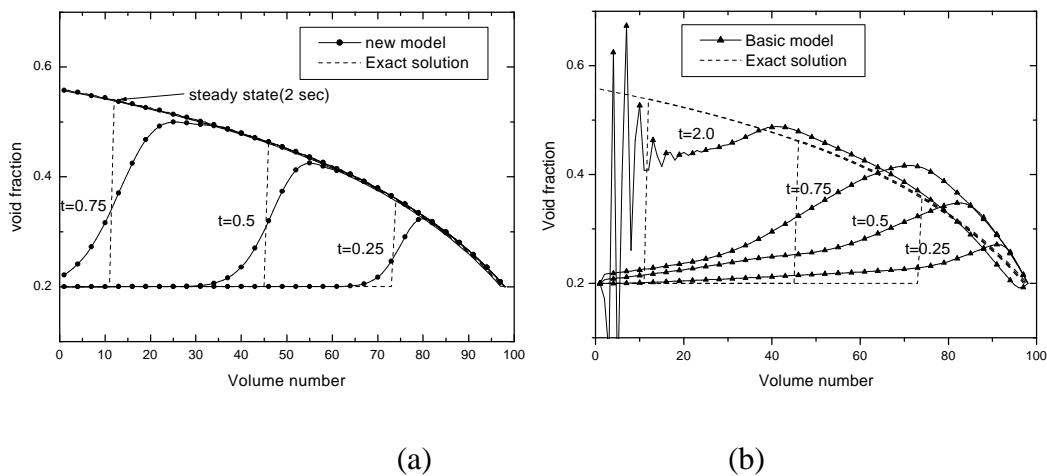


Figure 7 The Water Faucet Problem (a) New Model, (b) Basic Model

5. Concluding Remarks

In this paper, the numerical stability of Interfacial pressure force model was performed using a linearized Von-Neumann stability analysis for semi-implicit discretization scheme. It was shown that this model has smaller spectral radius than basic and virtual mass models under same physical condition. Also, in order to investigate the stability in the numerical calculation of this model, a pilot code was developed and applied for simulating wave

perturbation and faucet problems. In perturbation problem, perturbation wave in the present model is continuously damped out and finally disappears while other models result in numerical instabilities. In addition, in faucet test, this model showed good agreement with the exact solutions. Consequently, we can conclude that the present model has a more improved simulation capability than the basic two-fluid model and can be easily implemented in current nuclear safety analysis codes.

NOMENCLATURE

| | |
|-------------------|---|
| A | flow area |
| C_v | virtual mass coefficient |
| c | sonic speed |
| FIF | liquid interfacial friction coefficient |
| FIG | vapor interfacial friction coefficient |
| FWF | liquid wall friction coefficient |
| FWG | vapor wall friction coefficient |
| k | wave number |
| p | pressure |
| v | velocity |
| α | void fraction |
| Dx | volume length |
| Dt | time step size |
| Γ | vapor generation rate |
| ρ | mass density |
| Subscripts | |
| f | liquid phase |
| g | vapor phase |
| i | interface |
| m | mixture |

Superscripts

| | |
|---|-----------------------|
| n | time step advancement |
|---|-----------------------|

ACKNOWLEDGMENTS

This work was performed under the Long-term Nuclear R&D Program sponsored by the Ministry of Science and Technology

REFERENCES

1. Lyczkowski, R. W., Gidaspow, D., Solbrig, C.W., and Hughes, E. D., 1978, Characteristics and stability analysis of transient one-dimensional two-phase flow equations and their finite difference approximations, *Nucl. Sci. Eng.*, 66, 378.
2. Arai, M., 1980 "Characteristics and Stability Analysis for Two-Phase Flow Equation Systems with Viscous Terms," *Nucl. Sci. Eng.*, Vol. 74, pp. 77-83
3. Doster, J. M. and Holmes, M. A., 1996, Numerical stability of the six-equation, single-pressure model with viscous terms, *Nucl. Sci. Eng.*, 124, 125.
4. No, H. C. and Kazimi, M. S., 1985, Effects of virtual mass on the mathematical characteristics and numerical stability of the two-fluid model, *Nucl. Sci. Eng.*, 89, 197.
5. Ramshaw, J. D. and Trapp, J. A., 1978, Characteristics, stability, and short-wavelength phenomena in two-phase flow equation systems, *Nucl. Sci. Eng.*, 66, 93.
6. Stewart, H.B., 1979, Stability of two-phase flow calculation using two-fluid models, *J. Comput. Phys.*, 33, 259.
7. Stuhmiller, J.H., 1977, "The influence of Interfacial Pressure Forces on the Character of the Two-phase Flow model Equations," *Int. J. Multiphase Flow*, Vol. 3, pp. 551-560
8. Forge, A., Pochard, R., Porracchia, A., Miro, J., Sonnenburg, H. G., Steinhoff, F. and Teschendorff, V., 1988, Comparison of Thermal-Hydraulic Safety Codes for PWR Systems, Graham & Trotman, London, pp. 60-105.
9. Holmes, M. A., 1995, Stability of Finite Difference Approximations of Two Fluid, Two Phase Flow Equations, Ph.D. Thesis, NCSU, Raleigh.
10. Carlson, K. E., Riemke, R. A., Rouhani, S.Z., Shumway, R. W., and Weaver, W. L., RELAP5/MOD3 code manual volume 1: code structure, system models, and solution methods (draft), NUREG/CR-5535, EGG-2596, EG&G Idaho, Inc., June 1990.
11. Lee, S. J., Chang, K. S., and Kim, K. D., 1998, Pressure wave speeds from the characteristics of two fluids, two-phase hyperbolic equation system, *Int. J. Multiphase Flow*, 24, 855-866.
12. Ransom, V. H., 1979, "Faucet Flow, Oscilating Manometer, and Expulsion of Steam by Subcooled Water," Part 3, Numerical Benchmark Tests, *Multiphase Science and Technology*, Volume 3
13. Gose, G. C., Peterson, C. E., McFadden, J. H., Paulsen, M. P., McClure, J. A., Shatford, J. G., Moser, M. A., Johnson, D. L., Jensen, P. J., Westacott, J. L., RETRAN-02 code manual volume 1: theory and numerics, NP-1850-CCM-A, Electric Power Research Institute, December 1995.

14. Kim, K. D., Lee, S. J., Chang, W. P., Ha, E. J., Jeun, G. D., 1998, Numerical Stability Analysis of New Hyperbolic Equations for Two-Phase Flow, Proc. 6th International Conference on Nuclear Engineering, San Diego.
15. Strikwerda, J. A., 1989, Finite Difference Schemes and Partial Differential Equations, Wadsworth & Brooks/Cole Advanced Books & Software Pacific Grove, California.
16. TRAC-PF1/MOD1: An advanced best-estimate computer program for pressurized water reactor thermal-hydraulic analysis, NUREC/CR-3858, LA-10157-MS, Los Alamos National Laboratory, 1986.
17. H. G. Lim, "Development and Application of Stability Enhancing Interfacial Pressure Force model for Two-Phase Flow Equations", Ph.D. Thesis, SNU